Response of low-latitude ionospheric total electron content to the geomagnetic storm of 24 August 2005

Shweta Sharma,[1] P. Galav,[1] N. Dashora,[2] S. Alex,[3] R. S. Dabas,[4] and R. Pandey[1]

[1]   Response of low-latitude ionosphere to the geomagnetic storm of 24 August 2005 has been studied using total electron content (TEC) data obtained from the Global Positioning System (GPS) receivers. These studies were carried out using the receivers that were located (1) near the northern crest (~15°N mag. Lat.) of the equatorial ionization anomaly around 56°E, 74°E, and 102°E longitude and (2) from the northern crest of the ionization anomaly down to the magnetic equator in the longitude belt 75°E ± 3°E. These studies have been substantiated with the ground-based magnetometer data at Tirunelveli and Alibag, an equatorial and off equatorial station, respectively. The ground-based ionosonde data at New Delhi, a low-latitude station, have also been used to substantiate the TEC observations. The storm day TEC shows two well-defined humps at all stations wherein enhancements of the order of 80%–100% have been observed. While the first of the enhancements has been attributed to the prompt penetration electric field associated with an interplanetary electric field (IEF Ey) of about 35 mV/m, the other one has been attributed to the second episode of the prompt penetration electric field (IEF Ey ~ 20 mV/m) and abnormal equatorial plasma fountain in late evening hours, respectively. During the unsteady ring current conditions when the IMF Bz was still southward, penetration of a westward electric field has been inferred. Two peaks in foF_2 have been observed whose time of occurrence coincides with those of the humps in the low-latitude TEC. Results from stations having nearly the same magnetic latitude show that the ionospheric response, in terms of GPS TEC, to the prompt penetration electric fields is longitudinally independent. Formation of the first hump in TEC is progressively delayed in time from low to near-equatorial latitudes for stations in different magnetic latitudes along nearly the same longitude. However, its time of appearance at Diego Garcia, a station magnetically conjugate to Udaipur, is the same as that at Udaipur. The results also reveal the poleward expansion of the ionization anomaly due to the storm. Disturbance dynamoelectric fields have been inferred to be responsible for the suppressed plasma fountain, resulting in suppressed TEC values and equatorward contraction of the ionization anomaly on 25 August, compared to a reference quiet day.

1. Introduction

[2] Global Positioning System (GPS) is a very well established tool for the satellite based navigation and ground positioning. The ionospheric parameter which is of utmost importance for the GPS based communication is the total electron content (TEC) as the range error in the GPS signals is directly proportional to it. While sudden, large variations in TEC are an impediment to the GPS based navigation [*Basu et al.*, 2001b; *Lin et al.*, 2005; *Dashora et al.*, 2009], yet it has been extensively used as an important parameter for various ionospheric studies [e.g., *Rastogi and Klobuchar*, 1990]. These studies have become more relevant with the advent of GPS based navigation as the TEC is known to vary drastically during geomagnetic storms [*Ho et al.*, 1998; *Jakowski et al.*, 1999; *Maruyama et al.*, 2004; *Foster and Rideout*, 2005; *Dashora and Pandey*, 2007; *Dashora et al.*, 2009]. Geomagnetic storms present an extreme form of space weather affecting a vast region of space, from Earth's magnetosphere down to the ionosphere. Ionospheric response to the geomagnetic storms is quite varied as the electrodynamics, chemical composition and neutral wind circulation may be affected. Such changes may lead to enhancements or decrements in the ionospheric

[1]Department of Physics, Mohan Lal Sukhadia University, Udaipur, India.
[2]National Atmospheric Research Laboratory, Gadanki, India.
[3]Indian Institute of Geomagnetism, Navi Mumbai, India.
[4]National Physical Laboratory, New Delhi, India.

plasma density [e.g., *Maruyama et al.*, 2004; *Kumar et al.*, 2005; *Dashora and Pandey*, 2007; *Dashora et al.*, 2009].

[3] Geomagnetic storms are initiated due to the activities on the Sun, mainly by the flares and/or the coronal mass ejection (CME), when the solar wind velocity, temperature and density vary drastically, accompanied by significant changes in the north-south component of the interplanetary magnetic field (IMF B_z). The changes in ionospheric electrodynamics are mostly attributable to the disturbance electric fields generated during the storms. Two types of disturbance electric fields have been identified, namely, the prompt penetration fields (PPF) and the disturbance dynamo fields (DDF). The prompt penetration fields are transient in nature, having a rise and decay time of about 15 min and last for a period that is about an hour or so [*Gonzales et al.*, 1979; *Fejer and Scherliess*, 1997; *Fejer et al.*, 2007] and are felt nearly simultaneously over a wide range, from middle to equatorial latitudes [*Kikuchi et al.*, 1996, 2000; *Fejer et al.*, 2007]. The southward turning of IMF B_z from a steady northward configuration results in enhanced region 1 currents compared to those in the region 2 and results in the generation of the PPF [e.g., *Fejer*, 2002]. Similarly, when the IMF B_z turns northward from a large steady southward value, or decreases to zero from a large value, a PPF is generated which is opposite to the one generated due to the southward turning of the IMF B_z [e.g., *Kelley et al.*, 1979]. These two types of fields are also termed undershielding and overshielding electric fields, respectively, owing to their generation mechanisms. The undershielding fields are directed eastward (westward) during the day (night) at the equator [e.g., *Fejer*, 2002] whereas the converse holds for the overshielding fields [*Kelley et al.*, 1979], which are directed westward (eastward) during the day (night).

[4] The enhanced energy input and consequent Joule heating of the high-latitude atmosphere during the geomagnetic storms results in modification of the global thermospheric winds which generate the disturbance dynamo fields [*Blanc and Richmond*, 1980]. These fields are generated within a few hours of the storm and manifest on varied time scales, from a few hours to days [e.g., *Scherliess and Fejer*, 1997; *Richmond et al.*, 2003]. The direction of the DDF is opposite to the ambient zonal electric field at the equator [e.g., *Scherliess and Fejer*, 1997] and hence are directed westward (eastward) during the day (night).

[5] Impulsive energy inputs during the storms may result in the launching of TADs, the traveling atmospheric disturbances [*Hines*, 1960; *Balthazor and Moffett*, 1997] which travel meridionally toward equator at high speeds. The TADs drag the ionization along the geomagnetic field lines [*Kirchengast et al.*, 1996; *Sastri et al.*, 2000] and lead to a positive ionospheric storm. It has been shown recently [*Bruinsma and Forbes*, 2007] that TADs modulate the ionization, more during the night than during the day and the maximum amplitude of such modulations is nearly 25%.

[6] Electrodynamic effect of the disturbance fields is in terms of the modification of the equatorial fountain arising due to the **E** × **B** drift of plasma in the vertical direction. During the day, if the electric fields uplift the plasma at the equator, it survives longer due to slower recombination rates at higher altitudes. While at the lower altitudes photo ionization replenishes the plasma, there is an overall increase of the F region height and plasma [e.g., *Astafyeva*, 2009].

[7] Ionospheric effects of geomagnetic storms have been a subject of sustained study for several decades now [e.g., *Spiro et al.*, 1988; *Fejer et al.*, 1990; *Abdu et al.*, 1995; *Fejer*, 1997; *Sastri et al.*, 1997, 2002; *Basu et al.*, 2001a]. During the recent past, such studies have been carried out using the GPS derived TEC. In spite of so much effort in this direction, in a recent study, *Fejer et al.* [2007] have underlined incompleteness in the present-day understanding of the magnetosphere-ionosphere coupling processes that govern the dynamics of the low-latitude and equatorial ionosphere during the disturbed periods. This makes it imperative to study each storm event from multiple observation points to bring out all commonalities and differences with regard to a particular event. This is the motivation for the present study that concerns with the geomagnetic storm of 24 August 2005 which occurred during the local daytime. August 2005 was part of the declining phase of the solar cycle 23, with an average F10.7 cm solar flux of about 90.6 SFU but had periods of strong geomagnetic activity. One such period of increased activity was 22–28 August. The active region (AR) 10798 was responsible for the M2.6 and M5.6 flares on 22 August peaking at 0132 UT and 1727 UT, respectively. Both these flares were accompanied by halo CMEs (http://lasco-www.nrl.navy.mil) which were later detected as interplanetary disturbances by the ACE spacecraft as two shocks in quick succession. The 24 August 2005 geomagnetic storm was triggered due to the combined effects of these CMEs [*Papaioannou et al.*, 2009].

[8] For the study of this storm, we have made use of the TEC data from the 5 GPS receivers around the 75°E longitudes covering northern and southern edges of the equatorial ionization anomaly (EIA). Diego Garcia, a station in the southern hemisphere is almost magnetically conjugate to Udaipur. From this part of the globe, comparisons of results from two magnetically conjugate stations during a storm are being presented probably for the first time. Also, we have used TEC data from three GPS receivers around 15°N magnetic latitude, in different longitudes. We have also made use of ionosonde data from New Delhi, a station north of the EIA in the Indian region.

2. Data Sets

[9] Level 2 data of the ACE satellite, with a time resolution of 64 s, have been used to show the solar wind parameters such as proton density (N_P), proton temperature (T_P) and solar wind speed (V_{SW}). IMF B_z (in the GSM coordinates) values with a time resolution of 16 s has also been used from the same satellite. From these parameters the zonal component of the interplanetary electric field (IEF E_y) has been computed as, E_y (mV/m) = $-V_{SW} B_z$. The polar cap potential drop Φ_{PC}, has been calculated using the Hill-Siscoe polar cap formula [*Siscoe et al.*, 2002; *Ober et al.*, 2003; *Fejer et al.*, 2007], i.e.,

$$\Phi_{PC}(kV) = \frac{30 + 57.6 E_R P_{SW}^{-1/6}}{1 + 0.20 \Sigma_P P_{SW}^{-1/3} + 0.036 E_R P_{SW}^{-1/2} \Sigma_P}.$$

Here E_R (mV/m) = $V_{SW} B \sin^2(\theta/2)$, is the reconnection electric field, B(nT) is the Y-Z plane component of the IMF in GSM coordinates, and θ is the IMF clock angle in the Y-Z plane, with 0° and 180° correspond to northward and southward, respectively. A 30 kV potential has been included to

Table 1. List of GPS Stations Used for the Present Study

	Station Name	Station Code	Geographic Latitude	Geographic Longitude	Geomagnetic Latitude
1	Yibal, Oman	YIBL	22.18°N	56.11°E	15.8°N
2	Udaipur, India[a]	UDPR[a]	24.67°N	73.69°E	16.22°N
3	Kunming, China	KUNM	25.03°N	102.79°E	15.05°N
4	Hyderabad, India	HYDE	17.42°N	78.55°E	8.65°N
5	Bengaluru, India	IISC	13.02°N	77.57°E	4.35°N
6	Maldives, Republic of Maldives	MALD	4.18°N	73.53°E	4.18°S
7	Diego Garcia Island, U.K. Territory	DGAR	7.27°S	72.37°E	15.36°S

[a]Not an IGS station.

account for viscous merging and predicts saturation for large solar wind reconnection electric fields. P_{SW} (nPa) = N_P m_p V_{SW}^2, is the solar wind pressure, N_P is the solar wind number density, and m_p is the proton mass, and Σ_P = 0.77 $(F_{10.7})^{1/2}$ is the height integrated Pedersen conductivity.

[10] We have used the SYM-H and ASY-H indices which represent the strength of the symmetric ring currents and longitudinal symmetry of the ring currents, respectively.

[11] The magnetic field strength in the north-south direction measured by the ground-based magnetometers at Alibag (H_{ABG}), an off-equatorial station and at Tirunelveli (H_{TIR}), an equatorial station in Indian longitude sector have been used to describe the variations in the overhead currents. The difference $\Delta H_{TIR} - \Delta H_{ABG}$, is normally computed to show the strength of the equatorial electrojet (EEJ), where ΔH at each location is estimated after subtracting the respective average nighttime level from its H values. This subtraction is expected to eliminate the ring current contribution. However, during disturbed ring current conditions, this subtraction may not give a true EEJ contribution. This is because the ring current does have latitudinal dependence, as revealed by disturbed ASY-H parameter. Therefore, we have chosen to compute the difference, $\Delta H = H_{TIR}–H_{ABG}$ on the storm day (designated by ΔH_S) of 24 August and its variation has been compared with that on a quiet day (ΔH_Q). However, for 25 and 26 August, the quiet days, we shall follow the conventional procedure.

[12] Latitudinal and longitudinal extents of the ionospheric variations during the geomagnetic storm of 24 August 2005 have been studied. For this purpose the TEC data, obtained through the GPS receivers, of two sets have been considered. The first set consisted of stations that had nearly the same latitude, around the anomaly crest in the northern hemisphere, but different longitudes. The second one corresponded to different latitudes, from anomaly crest in the northern hemisphere to down to the equator, in the longitude belt 75°E ± 3°E (Local time, LT = UT + 5). List of such stations, along with respective geographic coordinates is given in Table 1. Except for Udaipur the rest of the stations listed in Table 1 are the IGS (International GNSS Service) stations, whose data have been downloaded from the site ftp://garner.ucsd.edu/. It is to be noted here that the IGS data are in RINEX (Receiver INdependent EXchange) format which have been read using indigenously developed computer codes. TEC at Udaipur has been computed from a GPS receiver, GSV 4004A of M/S GPS Silicon Valley, USA. The line-of-sight TEC (slant TEC, STEC) between a satellite receiver has been computed after resolving the initial ambiguity and correcting for the cycle slips in the RINEX formatted data. This slant TEC suffered from the satellite and receiver bias errors. These errors have been accounted for during post processing of data by downloading the bias errors from the site ftp://ftp.unibe.ch/aiub/. The corrected slant TEC has been converted into vertical TEC (VTEC) using the formula given by *Ma and Maruyama* [2003]. For this purpose a thin ionospheric shell at 350 km height has been assumed. Thus, the computed VTEC corresponds to the coordinates of the ionospheric pierce points.

$$VTEC = STEC \times \left[1 - \left(\frac{R_e \cos \theta}{R_e h_{max}} \right)^2 \right]^{1/2} \quad (1)$$

Here R_e is the radius of the Earth, θ is the elevation angle, and h_{max} is the height of the ionospheric shell above the surface of the Earth.

[13] The TEC data near the northern crest of the equatorial anomaly have been substantiated by ionosonde observations, that give variations of h_mF_2 and foF_2 over New Delhi (Geog. Lat. 28.64°N, Geog. Long. 77.17°E, and Geomagnetic latitude 19.94°N).

3. Results and Discussion

3.1. Solar Wind, IMF B_z, and Geomagnetic Data

[14] Variations in solar wind parameters N_P, T_P and V_{SW}, the IMF B_z, Φ_{PC}, IEF Ey, E_R and various geomagnetic parameters, SYM-H, ASY-H, and ΔH_S for the period 0100 UT to 1400 UT (0500 LT to 1900 LT, 75°E) on 24 August 2005 covering the local daytime have been shown in Figure 1 from the top to bottom image, respectively. In Figure 1 (bottom) the broken curve in red is the normal trend of (ΔH_Q) on a quiet day, with a maximum at 0600 UT. It can be seen from the curve that, compared to the nighttime level, the peak ΔH_Q is about 75 nT, corresponding to the normal contribution of the electrojet currents. The curve in blue is the ΔH_S variations on 24 August which are markedly different from its normal variation.

[15] For a better comparison of parameters obtained from the ACE satellite and ground-based instruments, the solar wind parameters and IMF B_z have been shifted in time by 35 min in accordance with the shock observed in the SYM-H index. It can be seen from Figure 1 that the solar wind velocity V_{SW} increased abruptly from 440 km/sec to about 550 km/sec at 0610 UT on 24 August 2005. A similar increase is also seen in solar wind temperature and density. This sudden enhancement in solar wind parameters raised the polar cap potential to a high value of ~200 kV. Correspondingly, the IEF Ey increased up to 8 mV/m for a short duration. Although the IMF B_z was steady, increased Φ_{PC} after 0615 UT points to enhancement of the region 1 currents
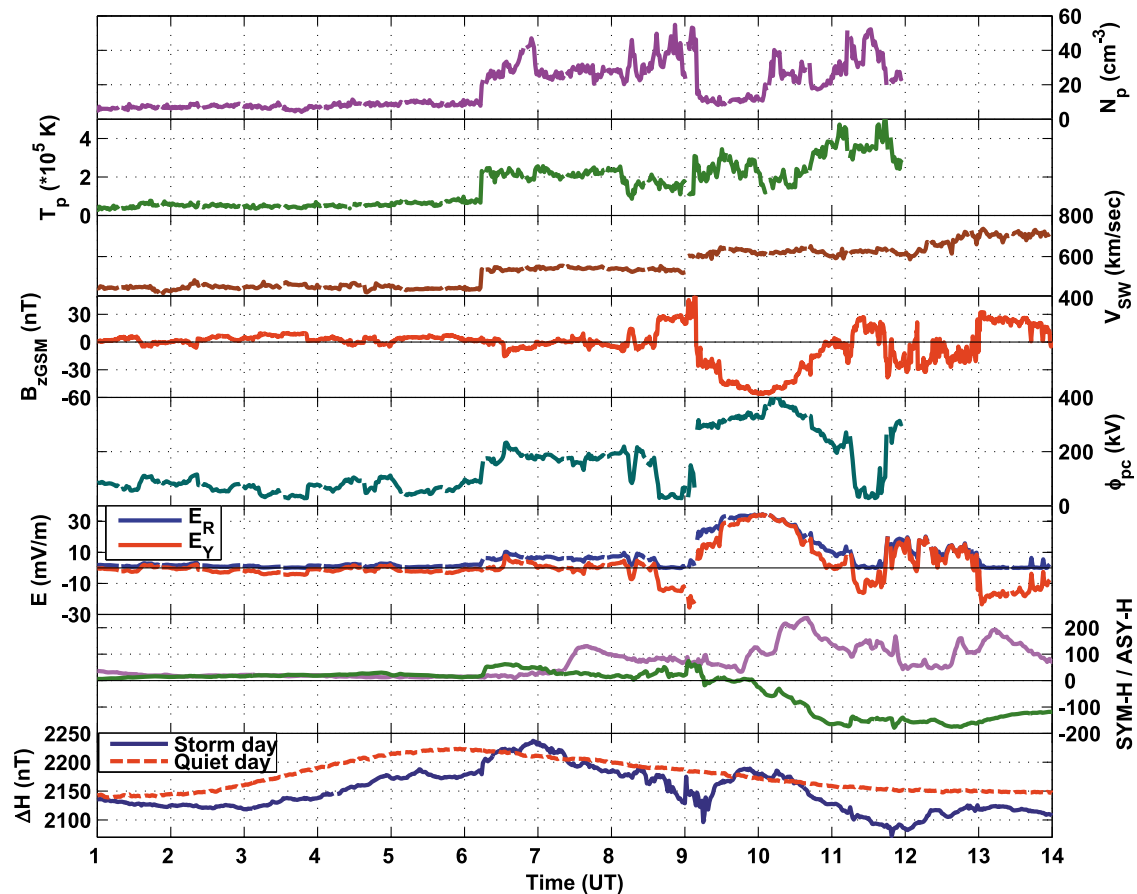
Figure 1. The solar wind density, temperature, speed, IMF B_z, cross polar potential drop, zonal interplanetary electric field (IEF Ey), reconnection electric field E_R, SYM-H and ASY-H indices, and ΔH variations on 24 August 2005.

resulting in increased geomagnetic activity, as evidenced in SYM-H. *Gonzalez et al.* [1992, 1999] have noted that an increase in ram pressure, signified by jumps in proton density and solar wind speed causes a sudden compression of the magnetosphere and results in a positive jump in the horizontal component of the Earth's magnetic field. This jump, also seen in the D_{st} or SYM-H as a positive jerk, has been termed a sudden impulse, or, SI. (The SI may, or may not, be followed by a storm main phase.)

[16] At around 0835 UT the IMF B_z suddenly increased to a northwardly value of ~30 nT. Concurrently, the Φ_{PC} dropped near zero and the IEF Ey decreased sharply to a value of ~−13 mV/m (westward). Further, at 0900 UT, an abrupt rise in V_{SW} up to 600 km/sec was accompanied by an impulsive rise in IMF B_z to a northward value of about 50 nT and positive jerks in SYM-H. Simultaneously, the IEF Ey further decreased to reach a maximum value of about −25 mV/m. The period from 0830 UT to 0910 UT may be taken as the initial phase of the storm. Thereafter, the IMF B_z turned southward which was associated with increased Φ_{PC} and eastward IEF Ey at around 0910 UT. This signaled the onset of the storm main phase wherein the SYM-H started declining. The IMF B_z attained a southwardly maximum of 55 nT at 1000 UT and the lowest SYM-H value was about −179 nT.

[17] The southward turning of IMF-B_z observed at 0910 UT created strong eastward interplanetary and reconnection electric fields, IEF Ey and E_R. These electric fields reached a maximum value of ~35 mV/m.

[18] Although not shown here, from 1000 UT onward the IMF By became westward and IMF Bz started recovering from its maximum southward value. At the same time, the solar wind ram pressure increased abruptly as revealed by its two peaks in N_P. Concurrent with increased ram pressure after 1000 UT, the ASY-H showed marked increase and reached up to 225 nT. Increased ASY-H index implies unsteady ring current condition. There are two more episodes of significant IMF Bz turnings; northward at 1115 UT and southward at 1145 UT, respectively. These turnings generated westward and eastward IEF Ey of some significance. The IMF Bz remained largely southward till about 1300 UT. Thereafter it turned polarity and remained largely northward.

[19] As shown in Figure 1 (bottom), ΔH variations on the storm day are markedly different from its quiet day variations. Even prior to the occurrence of magnetospheric disturbances, the ΔH is seen to be below the quiet day base values up to about 0400 UT. This is normally inferred as a counter electrojet signature. After 0400 UT, the ΔH_S recovered and started increasing compared to the base value of ΔH_Q. A sudden increase in RAM pressure signified by

increased N_p and V_{sw} at 0610 UT increases Φ_{pc} to ~200 kV. This produced a sudden impulse (SI) in SYM-H. Instantaneous effect is seen in SYM-H as it is a contribution of the ring current. A sudden rise in ΔH_S at 0610 UT is due to the SI. Around 0630 UT, IMF Bz turns southward to a value of about 20 nT. There is a positive kink in the Φ_{pc} and manifests itself as an increase in ΔH_S around 0645 UT. The ΔH_S peaked at 0700 UT, about an hour later than on a normal day. As noted above, the storm initial phase was from 0830 UT to 0910 UT wherein Bz became strong northward to a value of about 30 nT and there about for 30 min. Concurrently, the Φ_{PC} and E_R dropped near zero. This sudden northward turning of IMF Bz could lead to overshielding condition resulting in an overshielding electric field which would be westward during the day [e.g., *Kelley et al.*, 1979; *Wolf et al.*, 2007]. This westward electric field is seen to get transmitted to the equator with a time delay of about 10 min and probably as a result, the ΔH_S, which was in its declining phase past the local noon decreased more rapidly and reached a value of about 2100 nT at around 0915 UT. Thus a penetration of a westward electric field is inferred, due to which the ΔH_S declined rapidly. The source of this westward field observed in the dayside equatorial ionosphere during the northward Bz is the westward field of the shielding layer.

[20] Due to southward turning of IMF Bz, at 0910 UT, a strong eastward IEF Ey (of ~35 mV/m) was generated and an undershielding condition was developed. Simultaneously, ΔH_S increased abruptly by 90 nT, from 2100 nT to 2190 nT, within 35 min. A sudden increase of about 90 nT at a time when IEF Ey was also large and eastward implies eastward PPF resulting in enhanced overhead currents. A 90 nT increase in ΔH_S, caused by the eastward PPF is more in magnitude than the peak value (about 75 nT) of electrojet strength on a normal day. The undershielding conditions, which are responsible for the prompt penetration electric fields, usually last for a short duration [e.g., *Fejer et al.*, 2007]. Hence, after 1010 UT the ΔH_S decreased, as expected. However, its decrease below 2080 nT around 1150 UT is abnormal and cannot be explained merely by termination of the undershielding conditions. Such a large decrease in ΔH_S implies an additional westward PPF after about 1030 UT. In order to explain the source of an additional westward PPF, we invoke the hypothesis of *Fejer et al.* [2007] wherein they have argued unsteady ring currents to be a cause of eastward as well as westward PP electric fields. On 24 August, the ASY-H is seen to be high after 1000 UT, reaching a maximum around 1030 UT. The increased ASY-H around 1030 UT could have facilitated an additional westward PPF, under whose influence the ΔH_S declined rapidly. There was a northward turning of IMF Bz at 1115 UT. Prior to this northward IMF Bz, condition of southward IMF Bz prevailed. Thus, there was sudden change from the undershielding condition to the overshielding, resulting in the penetration of a westward field of the shielding layer. This westward field further decreased the ΔH_S up to about 2080 nT. An altogether different source of the abnormal westward field referred above, could be invoked from the work of *Ridley and Liemohn* [2002] wherein divergence of asymmetric ring current has been argued to be a source of PPF. Yet another source of such a westward field could be thought of arising due to the rapid disturbance dynamo fields reported

by *Fuller-Rowell et al.* [2002]. The basis of this DD field stems from slow variation in ΔH_S. These westward fields could reach low latitudes which result in downward plasma drift during the daytime. Such anomalous fields are expected during main and early recovery phases of the storms.

[21] Upturning of the ΔH_S from its second most negative value at 1150 UT may be attributed to the southward turning of the IMF B_z at 1145 UT. The Bz remains southward for over an hour past 1145 UT signifying an eastward IEF Ey (maximum value ~20 mV/m) which could penetrate to the low and equatorial latitudes as an eastward PPF. In spite of a large IEF E_y, its effect as seen in the ΔH_S variations does not appear to be commensurate. It is because the output of a ground-based magnetometer is a measure of overhead currents which in turn depend on electrical conductivities and electric fields. As the conductivities rapidly decrease past the local noon, even large changes in electric field strength would not be able to produce commensurate variations in the magnetic field strength. In other words, the effect of electric field seen in the ground-based magnetometers, around the local noon when the conductivities are normally high, would be much larger than that observed, say 3 h, past the local noon. After 1300 UT the ΔH_S tended to recover but was below the quiet time ΔH values.

3.2. Ionosonde Observation

[22] We have also studied the ionospheric variation in terms of critical frequency (foF_2) and peak height of ionospheric F_2 layer, (h_mF_2) using the ionosonde data from a low-latitude Indian station, i.e., New Delhi (Geog. Lat. 28.42°N, Geog. Long. 77.21°E, Geomagnetic Lat. 19.36°N). Variations of h_mF_2 and foF_2 on 24 August have been shown in Figure 2 as dots in red which have been fitted with a spline to fill the data gaps. Variation of both these parameters has been compared with that on the quiet days. The quiet day variation has been obtained from the mean of international geomagnetic quiet days of August 2005. The mean variations are drawn in magenta. In order to explain the variations in h_mF_2 in terms of the PPFs, we also give the IEF Ey variation on 24 August in Figure 2 (top). It can be seen from Figure 2 (middle) that on a normal quiet day, the h_mF_2 starts rising after the sunrise and peaks around 0700 UT (1200 LT) at an altitude of 325 km. Thereafter, it gradually lowers during the daytime to an altitude of about 250 km by the local evening hours. Similarly, on a quiet day the foF_2 starts increasing after the sunrise and peaks around 1000 UT (1500 LT) and thereafter it declines. Compared to this normal behavior, both foF_2 and h_mF_2 reveal two peaks on 24 August. The h_mF_2 is seen to rise gradually from about 0630 UT and reached up to 350 km around 0800 UT. At 0915 UT (1415 LT) the h_mF_2 rose sharply to reach a height of about 475 km at 1000 UT. This rise in height of F layer coincides with the enhanced IEF Ey, signifying transmission of an eastward PPF. Under the influence of this PP field, the *F* region rises by about 130 km in just 45 min (0915 UT to 1000 UT) implying an average vertical drift speed of about 48 m/s. After 1000 UT (1500 LT) h_mF_2 decreased rapidly as the undershielding conditions ceased to exist, and lowered to 320 km by 1130 UT (1630 LT). Thereafter, it started rising again from about 1145 UT and reached an altitude of 475 km at 1215 UT. Thereafter the F layer came down rapidly and by 1300 UT h_mF_2 attained its normal value. Comparing top and middle images of Figure 2,
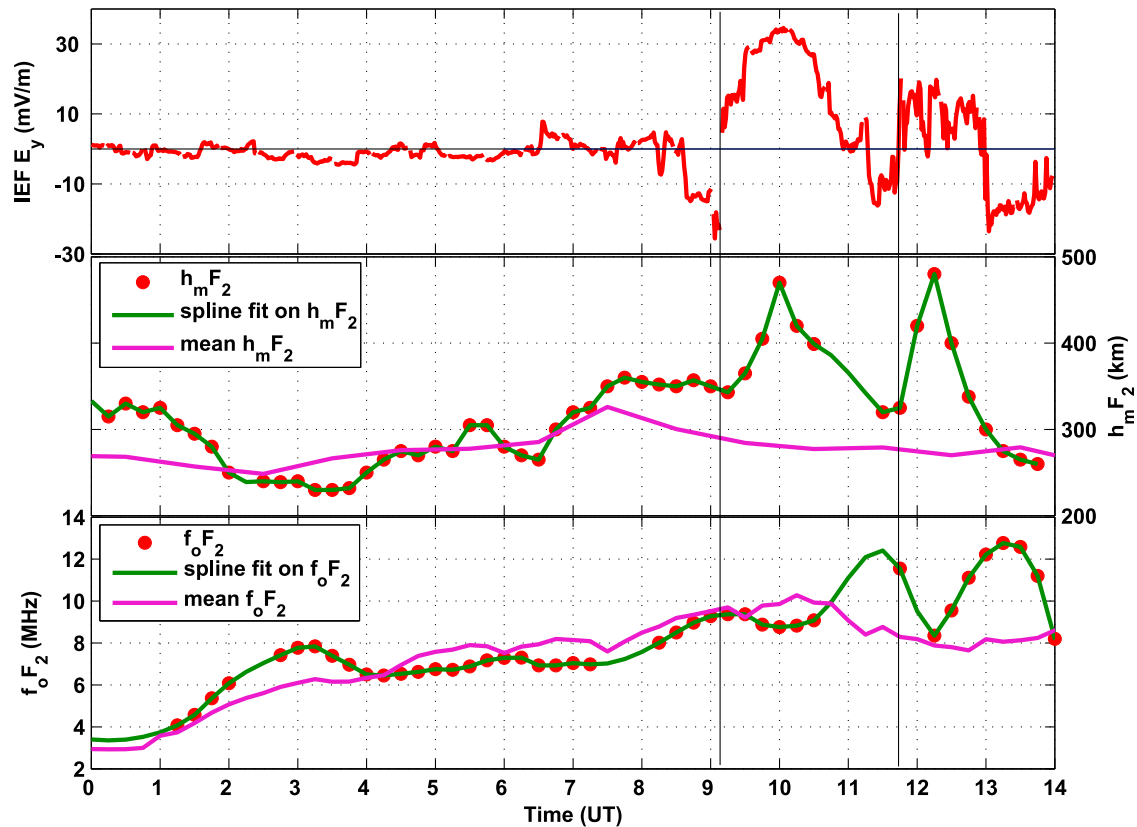
Figure 2. Variation of h_mF_2 and foF_2 at New Delhi on 24 August (red dots are the data values with a spline fit in green). Curve in magenta is the mean quiet day variation. Variations in h_mF_2 have been correlated with those in IEF Ey given in Figure 2 (top).

it can be seen that the second risetime of h_mF_2 nearly coincides with the occurrence of an eastward IEF Ey of 20 mV/m at 1145 UT, arising due to the southward turning of IMF Bz at 1145 UT. Thus, the rise in h_mF_2 could be explained in terms of eastward PP electric fields.

[23] That the geomagnetic storm led to a positive ionospheric storm is evidenced by a significant increase in the density, as revealed by peaks in foF_2 (Figure 2, bottom) around 1130 UT (1630 LT) and 1315 UT (1815 LT). As has been noted earlier, there was an eastward PPF at 0910 UT. This PP field is expected to penetrate up to low and equatorial latitude. Resultantly the vertical E × B drift would be enhanced. This enhanced E × B drift would uplift the low-altitude plasma to higher heights where the recombination rates are low and thus plasma would sustain for a longer time. Thus, the first peak in foF_2, observed at 1130 UT at New Delhi, could be attributed to the local uplifting of plasma by the enhanced vertical E × B drift arising due to the eastward PPF at 0910 UT (1410 LT) in the low latitudes, like New Delhi. Since the PP fields are expected to be short-lived, the foF_2 tended to attain its quiet day value at 1215 UT.

[24] From 1215 UT (1715 LT) the foF_2 again started increasing and peaked at 1315 UT (1815 LT). In order to understand the mechanism for the formation of the second peak in foF_2, it is pertinent to discuss the variation of foF_2 on a normal day at Delhi which is also given in Figure 2 as a curve in magenta. Formation of equatorial ionization anomaly (EIA) in low latitudes has been explained in terms

of plasma fountain that results due to vertical uplifting of plasma at the geomagnetic equator due to the **E** × **B** drift [*Martyn*, 1955; *Hanson and Moffett*, 1966] and its subsequent dumping at the low latitudes. It can be seen from Figure 2 that on a normal day, the foF_2 increases monotonically and reaches a maximum by about 1000 UT (1500 LT). The normal hour of maximization of EEJ at the equator is around 0600 UT (1100 LT). Thus, on a normal day the peak in foF_2 at a low-latitude station New Delhi, occurs nearly 4 h after the electrojet currents at the equator maximize. Hence the second peak in foF_2 at New Delhi could be attributed to two factors. The first of which is the equatorial plasma fountain arising due to the eastward PP electric field at the equator at 0910 UT. Under the influence of this PP electric field at the equator, the equatorial plasma rose to higher altitudes and then diffused along the field lines until the gravity and pressure gradient forces balanced. This contributed to the anomalous, second peak in foF_2 at 1315 UT in low latitudes, like New Delhi. The other factor that could also contribute to the second peak is the second episode of eastward PP electric field that occurred at 1145 UT (1645 LT). Due to this PP field, the local uplifting of plasma in the low latitudes resulted. These two factors, namely, the abnormal plasma fountain and the local uplift of plasma due to the eastward PP field at 1145 UT, combined together to produce the second peak in foF_2. Since the time of second episode of PPF is within the period of dumping of plasma due to the equatorial fountain arising from the first episode of PPF, it is
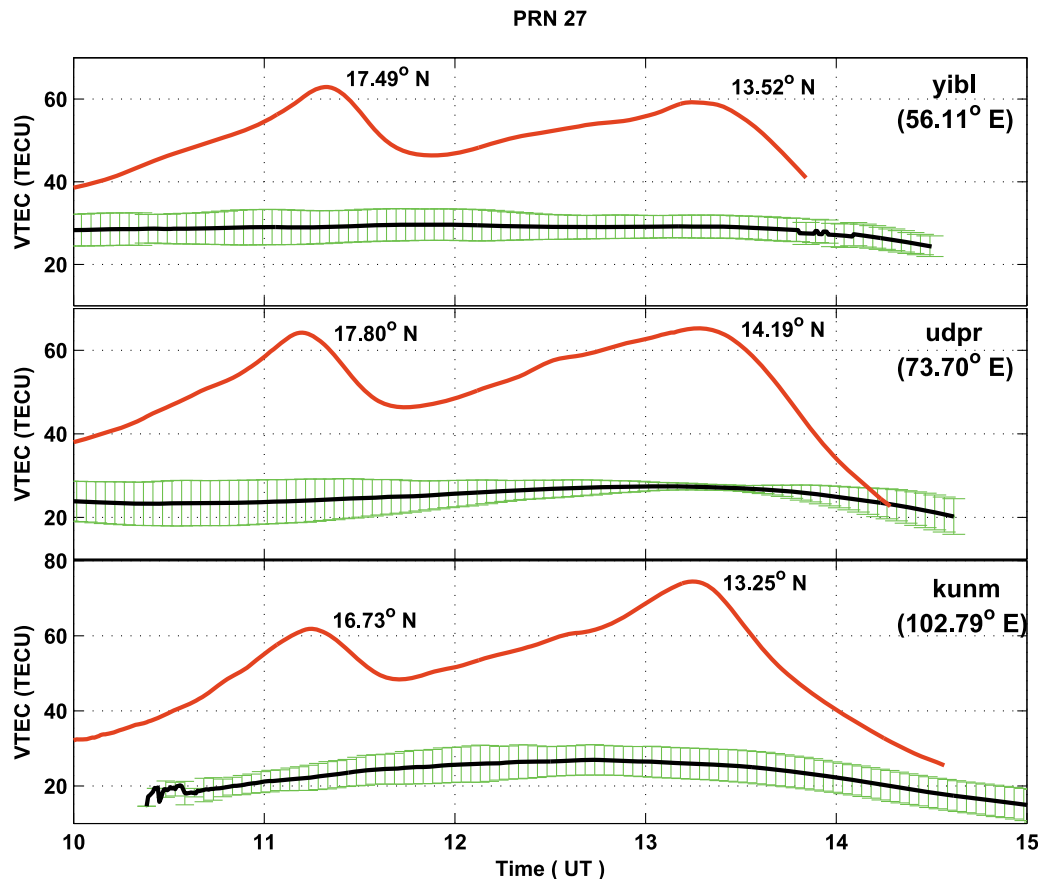
Figure 3. Variation of storm day VTEC (in red) for PRN 27 over Yibal, Udaipur, and Kunming. These stations have nearly the same magnetic latitude but differing longitudes. The quiet day mean VTEC for the same PRN is plotted in black with 2σ variations in green. The ionospheric pierce point latitude (magnetic) of each peak is also shown.

not possible to quantify and separate the contribution from the two sources. After 1815 LT, foF_2 started decreasing and reached its normal value by about 1400 UT (1900 LT).

3.3. Ionospheric TEC Variations

[25] In order to assess the effect of the geomagnetic storm on the ionospheric TEC, we have considered data from two sets of GPS stations. The first of these was along nearly the same latitude (but different longitudes) near the crest of the EIA and the other set enabled latitudinal TEC variation along nearly the same longitude in the Indian zone. Results for these sets are discussed in sections 3.3.1 and 3.3.2.

3.3.1. Longitudinal Variations in TEC

[26] Figure 3 gives variations in TEC for the GPS satellite designated with PRN 27 for three different stations, namely Yibal, Udaipur and Kunming, that have nearly the same geographic (magnetic) latitude, ~25°N (~16°N), but different longitudes, from 55°E to 105°E. Coordinates of these stations are given in Table 1. The curves in black give the mean quiet day variation in TEC and the band in green over it marks its day-to-day variability, 2σ bounds. The curves in red give the TEC variations for 24 August 2005 at these stations. It can be seen from Figure 3 that on 24 August, two well-separated humps in TEC are observed at all the three stations. The TEC starts to rise from 1000 UT and shows the

first hump around 1115 UT, 2 h past to the southward turning of the IMF Bz at 0910 UT. The TEC values are observed to be enhanced by a factor of two compared to its quiet day mean value. The second hump is seen around 1315 UT with an enhancement of ~30 TECU compared to the mean VTEC, at all the three longitudes. The time of occurrence of both the humps nearly coincides with that of the peaks in foF_2 as given in Figure 2. The fact that the humps in VTEC are seen nearly simultaneously at all the three stations lying in the same latitude but different longitudes, imply a common mechanism for their formation. Since the TEC is the integrated ionospheric plasma density which is heavily weighted by the F region density, variations in TEC are expected to be similar to those observed in foF_2 which is a measure of maximum plasma density of the F region. Thus, the mechanisms, namely the PP electric fields and/or abnormal plasma fountain, which were invoked to explain the peaks in foF_2 observed at New Delhi could be applied to explain the humps in VTEC which have been observed at stations around the northern crest of EIA having different longitudes.

[27] The results of this case also imply that on the dayside of the globe where nearly similar ionospheric conditions prevail, the ionospheric response to the PP electric fields does not show longitudinal dependence.
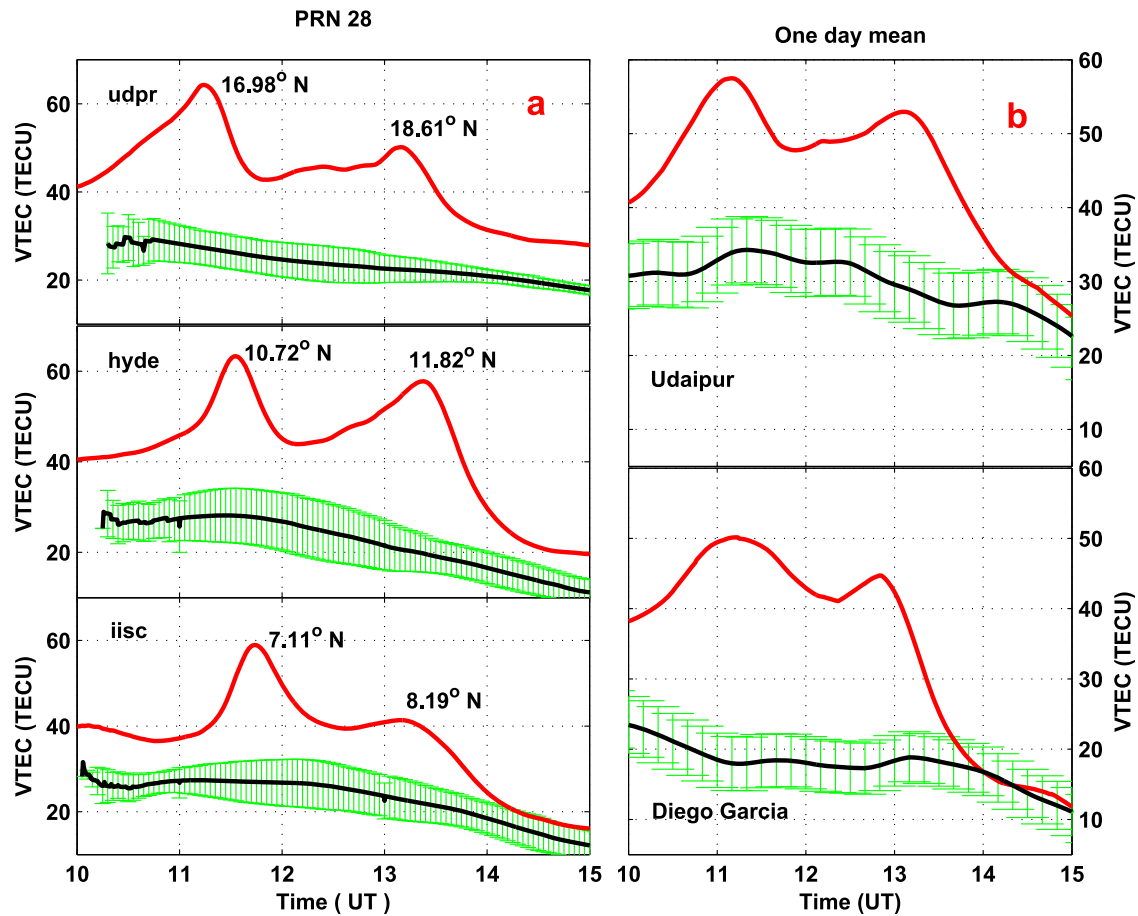
Figure 4. (a) Variation of storm day VTEC (in red) for PRN 28 over Udaipur, Hyderabad, and Bengaluru. These stations are in 75°E ± 3°E longitude (Local Time, LT = UT + 0500, at 75°E) from near the anomaly crest down to the equator. The quiet day mean VTEC for the same PRN is plotted in black with 2σ variations in green. The ionospheric pierce point latitude (magnetic) of each peak is also shown. (b) Temporal variation of mean VTEC on 24 August (in red) over Udaipur and Diego Garcia. These stations are geomagnetically conjugates, situated near the anomaly crest in northern and southern hemispheres, respectively. The quiet day mean VTEC (in black) with 2σ variations (in green) is given for comparison.

3.3.2. Latitudinal Variations in TEC

[28] We have also studied latitudinal variations in TEC from anomaly crest region in the northern hemisphere down to near equatorial stations that lie within 75°E ± 3°E (Local Time, LT = UT + 0500, at 75°E) longitude. These stations are Udaipur, Hyderabad and Bengaluru, whose coordinates are given in Table 1. Figure 4a gives variations in VTEC for these stations computed from the observations of the GPS satellite with PRN number 28. The curves in red show variations in VTEC on 24 August and the ones in black are the corresponding quiet time mean VTEC. Day-to-day variability is shown by scatter in green. It can be seen from Figure 4a that, on 24 August, the VTEC shows a double humped structure at all the stations. These humps are seen to be very distinct from the mean TEC. The time of occurrence of the first hump at Udaipur is around 1115 UT and it is delayed progressively as one goes down in latitude; the one at Bengaluru occurs around 1145 UT. As was observed at different longitudes, the VTEC is enhanced by about a factor of 2 at all these stations. The second hump in VTEC occurs at around 1315 UT. As noted in section 3.3.1, the

first hump in VTEC is due to the eastward PP electric field. There are differences with regard to its time of occurrence at different latitudes. We infer that these differences could be due to varying response of ionosphere to the PP electric field at different latitudes. To support this inference, we also give a plot of VTEC obtained from an IGS station at DGAR, Diego Garcia (7.2°S, 72.4°E, Geomag. Lat. 15.5°S), which is in the southern hemisphere and is nearly magnetic conjugate to Udaipur. Since, the same satellites could not be in view at the two stations at the same time, we give a profile of VTEC, computed using 30 min mean of data from various satellites in view at the two stations, Udaipur and Diego Garcia in Figure 4b in red. The curves in black are the quiet day mean variation of VTEC at the two stations and the scatter in green gives its day-to-day variability. As was the case with Figure 4a, the VTEC variation at Diego Garcia also has two humps. The time of occurrence of the first hump at Diego Garcia is nearly the same as that at Udaipur. That is, the process for the formation of humps at the two stations is same. This observation of occurrence of the first hump in VTEC at nearly the same time at magnetically
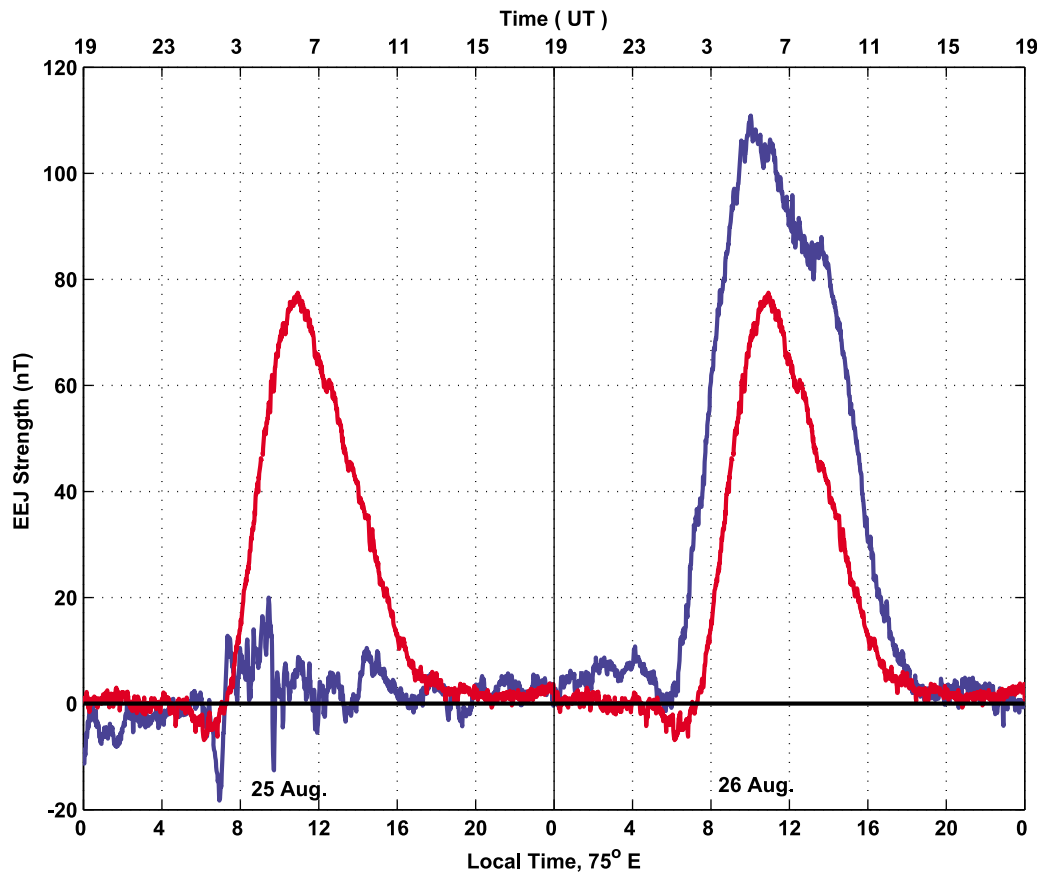
Figure 5. Variation of EEJ strength (in blue) for 25–26 August 2005. Curve in red shows its variation on a quiet day.

conjugate stations itself excludes the possibility of TAD being the cause of the manifestation of the first hump.

[29] The second hump in VTEC at different stations of Figures 4a and 4b, is due to the combined effect of the abnormal equatorial fountain and the eastward PP electric field at 1145 UT, as discussed in section 3.2. In terms of the peak value of TEC, the fountain is expected to have maximum effect at the anomaly crest and its efficiency diminishes with decreasing latitude. At the equator, it contributes to the formation of a shallow trough at the time when it creates a crest at higher latitudes. For the same reason, the second peak is poorly developed at Bengaluru. During the low solar activity phase, the EIA crest in the Indian zone has been shown to shift equatorward [*Galav et al.*, 2010], around 11°N. Hence, Udaipur is beyond the northern crest of the anomaly. The second peak shows maximum VTEC at Hyderabad when compared to Udaipur and Bengaluru. Hence, it can be concluded that the abnormal storm time fountain arising due to eastward PP electric fields at 0910 UT, has produced the ionization anomaly in the low latitudes in unusual late evening hours. Its crest lies between Udaipur and Bengaluru, probably over Hyderabad.

3.4. Disturbance Dynamo Effects

[30] Disturbance dynamo [*Blanc and Richmond*, 1980] effects are believed to be operational from a few hours to several hours after the storm commencement [*Fejer et al.*, 1983; *Scherliess and Fejer*, 1997]. Hence, their effects are to be felt on similar time scales. As has been noted in section 1, the disturbance dynamo arises due to change in wind circulation patterns and the dynamo fields thus generated are in opposition to the ambient electric fields at the equator, both during the day and night. We use the difference $\Delta H_{TIR} - \Delta H_{ABG}$ on quiet days, as a measure of the EEJ strength in relation to the VTEC observation on 25 and 26 August, as those were the quiet days. A plot of EEJ strength on 25 and 26 August has been given in Figure 5. The normal quiet time variation in EEJ strength has been overplotted in red for easy comparison. It can be seen from Figure 5 that on 25 August, the EEJ strength is greatly suppressed, by about 60 nT, compared to the normal day, with an average value of about 10 nT. Although not shown here, there were no significant variations in the daytime of 25 August either in solar wind parameters or, in AE index and IMF B$_z$. Thus, as there was no interplanetary disturbance on this day, the suppressed EEJ on 25 August may be attributed to the daytime westward electric field, arising due to the DDF. *Scherliess and Fejer* [1997] and *Fejer* [2002] indeed discuss the long-term component of the disturbance dynamo that manifest with time delays of 20–30 h. The strength of these disturbance fields would, probably, depend upon the strength of the solar event that preceded it, coupled with the conductivity distribution in the equatorial ionosphere.

[31] In contrast to the EEJ variations of 25 August, the ones on 26 August show a significant increase, by about 30 nT compared to the normal peak value. While the source
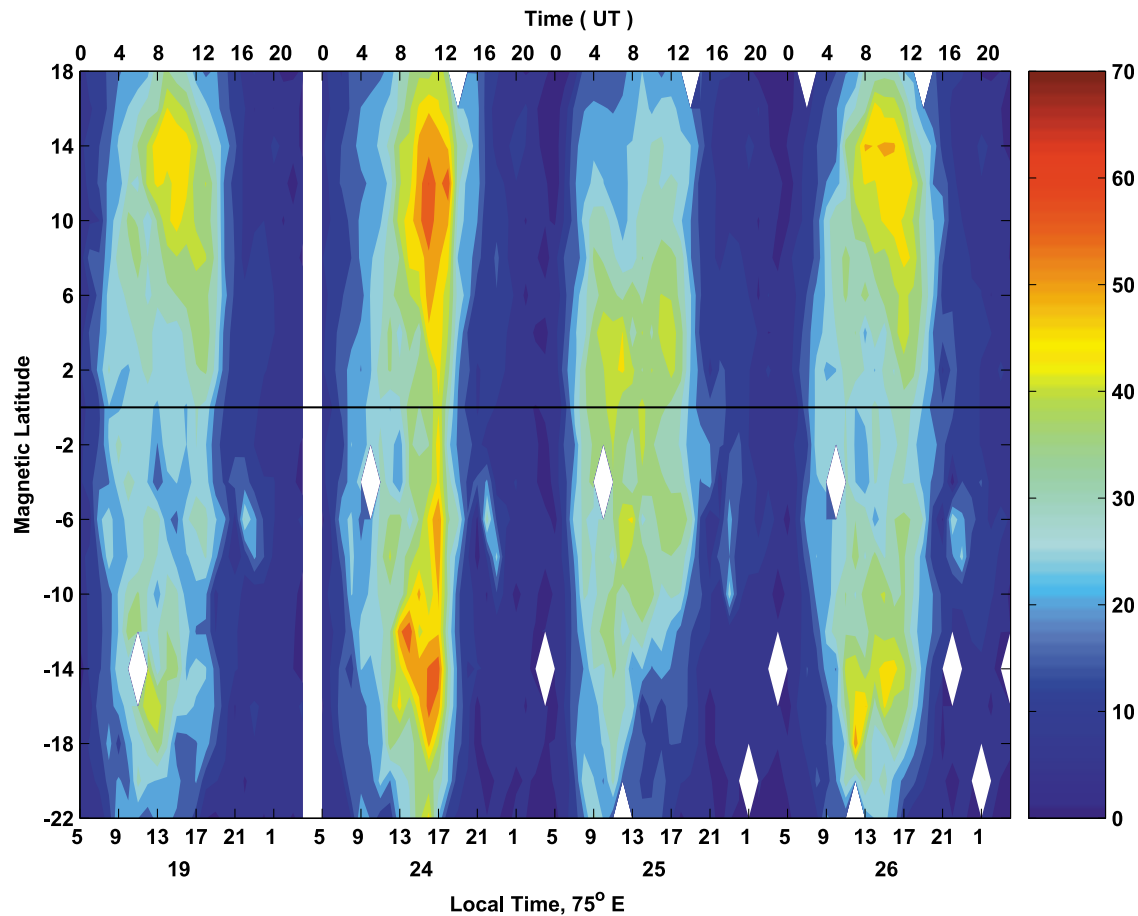
Figure 6. Contour map of VTEC with respect to time and magnetic latitude within the longitude belt of 75°E ± 3°E for 19 August, a reference quiet day, and 24–26 August. Strengthening and latitudinal expansion of equatorial anomaly on 24 August is clearly seen. Suppressed ionization anomaly on 25 August is also obvious.

of enhancement in the EEJ strength could not be ascertained, its effect on TEC are still useful to investigate. Relationship between the low-latitude TEC and the EEJ strength could be easily demonstrated through the variations of the former on 24 to 26 August, vis-à-vis that on 19 August, a quiet day. These TEC variations are shown in Figure 6 which gives latitudinal variations of TEC against time as contour plots. For this plot from Udaipur and four IGS stations namely, HYDE, IISC, MALD (Maldives), and DGAR have been used. On the control (quiet) day of 19 August, the TEC values are seen to maximize in a small band of latitude, 8°N–14°N and 12°S–16°S, around 1400 h, local time in the two hemispheres. In contrast to these quiet time variations, the TEC on 24 August is greatly enhanced and shows poleward expansion of the anomaly to both sides of the equator. As has been noted in earlier sections, this is due to the PP electric fields on 24 August. This result on poleward expansion of EIA due to PP electric field is in agreement with the earlier works [e.g., *Tsurutani et al.*, 2004]. Compared to the control day of 19 August, normal formation of EIA is seen to be inhibited on August 25. There are no well-defined crests in either hemisphere at the normal locations and there is a clear-cut reduction in TEC beyond ±8° latitudes. This is due to a weak fountain, as confirmed by

diminished EEJ strength on 25 August in Figure 5. Since the fountain was weak, the dumping of plasma was limited to latitudes very near the equator. Since there is no well-defined peak in EEJ strength on 25 August, the EIA could not develop and the TEC is confined to low latitudes. In contrast, the TEC on 26 August (Figure 6) shows latitudinal expansion arising due to enhanced EEJ strength. The TEC values are also higher compared to the control day.

4. Conclusions

[32] We have studied the response of low-latitude ionosphere to the geomagnetic storm of 24 August 2005 in terms of variations in TEC. For this study, we have made use of solar wind parameters, interplanetary magnetic field and data from ground-based magnetometers and ionosonde. Salient features of this study are as follows.

[33] 1. We have been able to discern the effect of eastward prompt penetration electric fields associated with increased cross polar potential drop and southward turning of IMF B_z on the TEC: along same latitude near the anomaly crest but with longitudes varying from 55°E to 105°E and along different magnetic latitudes from 16°N to 4°S, in the longitude belt 75°E ± 3°E.

[34] 2. The observed VTEC on the storm day shows ~80%–100% enhancement for all the studied stations, in the form of two humps.

[35] 3. The first hump in TEC has been attributed to the prompt penetration of electric field due to southward turning of IMF Bz at 0910 UT. Whereas the second hump at all the stations is found due to the combined effect of the PP field at 1145 UT and the abnormal plasma fountain arising from the first episode of PP electric field.

[36] 4. Two peaks in h_mF_2 on the storm day confirm the two episodes of eastward PP electric fields.

[37] 5. During the unsteady ring current conditions when the IMF Bz was still southward, penetration of a westward electric field has been inferred from the ground-based magnetometer data.

[38] 6. The response of low-latitude ionosphere to the storm time penetration of electric field does not seem to have any longitudinal dependence as evidenced by the simultaneous occurrence of the humps in TEC over ~55°E to ~105°E longitudes at nearly the same latitude.

[39] 7. There is a time delay in the occurrence of the first hump in the VTEC from low to equatorial latitudes. While its mechanism is to be understood, it could be attributed to the latitudinal ionospheric response to the PP field.

[40] 8. Storm day variations of foF$_2$, observed from New Delhi, are found to be similar to the variations of low-latitude VTEC.

[41] 9. Diminished TEC on 25 August (compared to the control day, 19 August) could be attributed to the disturbance dynamo fields leading to the weak EEJ that resulted in suppressed equatorial fountain.

References

Abdu, M. A., I. S. Batista, G. O. Walker, J. H. A. Sobral, N. B. Trivedi, and E. R. de Paula (1995), Equatorial ionospheric electric field during magnetospheric disturbances: Local/longitudinal dependencies from recent EITS campaigns, *J. Atmos. Terr. Phys.*, *57*, 1065–1083, doi:10.1016/0021-9169(94)00123-6.

Astafyeva, E. (2009), Effects of strong IMF B$_z$ southward events on the equatorial and mid-latitude ionosphere, *Ann. Geophys.*, *27*, 1175–1187, doi:10.5194/angeo-27-1175-2009.

Balthazor, R. L., and R. J. Moffett (1997), A study of atmospheric gravity waves and traveling ionospheric disturbances at equatorial latitudes, *Ann. Geophys.*, *15*, 1048–1056, doi:10.1007/s00585-997-1048-4.

Basu, S., S. Basu, K. M. Groves, H.-C. Yeh, S.-Y. Su, F. J. Rich, P. J. Sultan, and M. J. Keskinen (2001a), Response of the equatorial ionosphere in the South Atlantic Region to the Great Magnetic Storm of July 15, 2000, *Geophys. Res. Lett.*, *28*, 3577–3580, doi:10.1029/2001GL013259.

Basu, S., et al. (2001b), Ionospheric effects of major magnetic storms during the International Space Weather Period of September and October 1999: GPS observations, VHF/UHF scintillations, and in situ density structures at middle and equatorial latitudes, *J. Geophys. Res.*, *106*, 30,389–30,413, doi:10.1029/2001JA001116.

Blanc, M., and A. D. Richmond (1980), The ionospheric disturbance dynamo, *J. Geophys. Res.*, *85*, 1669–1686, doi:10.1029/JA085iA04p01669.

Bruinsma, S. L., and J. M. Forbes (2007), Global observation of traveling atmospheric disturbances (TADs) in the thermosphere, *Geophys. Res. Lett.*, *34*, L14103, doi:10.1029/2007GL030243.

Dashora, N., and R. Pandey (2007), Variations in total electron content near the crest of the equatorial ionization anomaly during the November 2004 geomagnetic storm, *Earth Planets Space*, *59*, 127–131.

Dashora, N., S. Sharma, R. S. Dabas, S. Alex, and R. Pandey (2009), Large enhancements in low latitude total electron content using 15 May 2005 geomagnetic storm in Indian zone, *Ann. Geophys.*, *27*, 1803–1820, doi:10.5194/angeo-27-1803-2009.

Fejer, B. G. (1997), The electrodynamics of the low-latitude ionosphere: Recent results and future challenges, *J. Atmos. Sol. Terr. Phys.*, *59*, 1465–1482, doi:10.1016/S1364-6826(96)00149-6.

Fejer, B. G. (2002), Low latitude storm time electrodynamics, *J. Atmos. Sol. Terr. Phys.*, *64*, 1401–1408, doi:10.1016/S1364-6826(02)00103-7.

Fejer, B. G., and L. Scherliess (1997), Empirical models of storm time equatorial electric fields, *J. Geophys. Res.*, *102*, 24,047–24,056, doi:10.1029/97JA02164.

Fejer, B. G., M. F. Larsen, and D. T. Farley (1983), Equatorial disturbance dynamoelectric fields, *Geophys. Res. Lett.*, *10*, 537–540, doi:10.1029/GL010i007p00537.

Fejer, B. G., R. W. Spiro, R. A. Wolf, and J. C. Foster (1990), Latitudinal variation of perturbation electric fields during magnetically disturbed periods: 1986 SUNDIAL observation and model results, *Ann. Geophys.*, *8*, 441–454.

Fejer, B. G., J. W. Jensen, T. Kikuchi, M. A. Abdu, and J. L. Chau (2007), Equatorial ionospheric electric fields during the November 2004 magnetic storm, *J. Geophys. Res.*, *112*, A10304, doi:10.1029/2007JA012376.

Foster, J. C., and W. Rideout (2005), Mid-latitude TEC enhancements during the October 2003 superstorm, *Geophys. Res. Lett.*, *32*, L12S04, doi:10.1029/2004GL021719.

Fuller-Rowell, T. J., G. H. Millward, A. D. Richmond, and M. V. Codrescu (2002), Storm-time changes in the upper atmosphere at low latitudes, *J. Atmos. Sol. Terr. Phys.*, *64*, 1383–1391, doi:10.1016/S1364-6826(02)00101-3.

Galav, P., N. Dashora, S. Sharma, and R. Pandey (2010), Characterization of low latitude GPS-TEC during very low solar activity phase, *J. Atmos. Sol. Terr. Phys.*, *72*, 1309–1317, doi:10.1016/j.jastp.2010.09.017.

Gonzales, C. A., M. C. Kelley, B. G. Fejer, J. F. Vickrey, and R. F. Woodman (1979), Equatorial electric fields during magnetically disturbed conditions: 2. Implications of simultaneous auroral and equatorial measurements, *J. Geophys. Res.*, *84*, 5803–5812, doi:10.1029/JA084iA10p05803.

Gonzalez, W. D., A. L. Clúa de Gonzalez Jr., O. Mendes, and B. T. Tsurutani (1992), Difficulties in defining storm sudden commencements, *Eos Trans. AGU*, *73*(16), 180, doi:10.1029/91EO00148.

Gonzalez, W. D., B. T. Tsurutani, and A. L. Clúa De Gonzalez (1999), Interplanetary origin of geomagnetic storms, *Space Sci. Rev.*, *88*, 529–562, doi:10.1023/A:1005160129098.

Hanson, W. B., and R. J. Moffett (1966), Ionization transport effects in the equatorial F region, *J. Geophys. Res.*, *71*, 5559–5572.

Hines, C. O. (1960), Internal atmospheric gravity waves at ionospheric heights, *Can. J. Phys.*, *38*, 1441–1481.

Ho, C. M., A. J. Mannucci, L. Sparks, X. Pi, U. J. Lindqwister, B. D. Wilson, B. A. Iijima, and M. J. Reyes (1998), Ionospheric total electron content perturbations monitored by the GPS global network during two northern hemisphere winter storms, *J. Geophys. Res.*, *103*, 26,409–26,420, doi:10.1029/98JA01237.

Jakowski, N., S. Schlter, and E. Sardon (1999), Total electron content of the ionosphere during the geomagnetic storm on 10 January 1997, *J. Atmos. Sol. Terr. Phys.*, *61*, 299–307, doi:10.1016/S1364-6826(98)00130-8.

Kelley, M. C., B. G. Fejer, and C. A. Gonzales (1979), An explanation for anomalous ionospheric electric fields associated with a northward turning of the interplanetary magnetic field, *Geophys. Res. Lett.*, *6*, 301–304, doi:10.1029/GL006i004p00301.

Kikuchi, T., H. Luhr, T. Kitamura, O. Saka, and K. Schlegel (1996), Direct penetration of the polar electric field to the equator during a *DP*2 event as detected by the auroral and equatorial magnetometer chains and the EISCAT radar, *J. Geophys. Res.*, *101*, 17,161–17,173, doi:10.1029/96JA01299.

Kikuchi, T., H. Liihr, K. Schlegel, H. Tachihara, M. Shinohara, and T.-I. Kitamura (2000), Penetration of auroral electric fields to the equator during a substorm, *J. Geophys. Res.*, *105*(A10), 23,251–23,261, doi:10.1029/2000JA900016.

Kirchengast, G., K. Hocke, and K. Schlegel (1996), The gravity wave-TID relationship: Insight via theoretical model—EISCAT data comparison, *J. Atmos. Terr. Phys.*, *58*, 233–243, doi:10.1016/0021-9169(95)00032-1.

Kumar, S., H. Chandra, and S. Sharma (2005), Geomagnetic storms and their ionospheric effects observed at the equatorial anomaly crest in the Indian region, *J. Atmos. Sol. Terr. Phys.*, *67*, 581–594, doi:10.1016/j.jastp.2004.12.003.

Lin, C. H., A. D. Richmond, J. Y. Liu, H. C. Yeh, L. J. Paxton, G. Lu, H. F. Tsai, and S.-Y. Su (2005), Large-scale variations of the low-latitude ionosphere during the October–November 2003 superstorm: Observational results, *J. Geophys. Res.*, *110*, A09S28, doi:10.1029/2004JA010900.

Ma, G., and T. Maruyama (2003), Derivation of TEC and estimation of instrumental biases from GEONET in Japan, *Ann. Geophys.*, *21*, 2083–2093, doi:10.5194/angeo-21-2083-2003.

Martyn, D. F. (1955), Theory of height and ionization density changes at the maximum on a Chapman-like region, taking account of ion production, decay, diffusion and total drift, in *Proceedings Cambridge Conference*, pp. 254–259, Phys. Soc. London, London.

Maruyama, T., G. Ma, and M. Nakamura (2004), Signature of TEC storm on 6 November 2001 derived from dense GPS receiver network and ionosonde chain over Japan, *J. Geophys. Res.*, *109*, A10302, doi:10.1029/2004JA010451.

Ober, D. M., N. C. Maynard, and W. J. Burke (2003), Testing the Hill model of transpolar potential saturation, *J. Geophys. Res.*, *108*(A12), 1467, doi:10.1029/2003JA010154.

Papaioannou, A., H. Mavromichalaki, E. Eroshenko, A. Belov, and V. Oleneva (2009), The burst of solar and geomagnetic activity in August–September 2005, *Ann. Geophys.*, *27*, 1019–1026, doi:10.5194/angeo-27-1019-2009.

Rastogi, R. G., and J. A. Klobuchar (1990), Ionospheric electron content within the equatorial anomaly belt, *J. Geophys. Res.*, *95*, 19,045–19,052, doi:10.1029/JA095iA11p19045.

Richmond, A. D., C. Peymirta, and R. G. Roble (2003), Long-lasting disturbances in the equatorial ionospheric electric field simulated with a coupled magnetosphere-ionosphere-thermosphere model, *J. Geophys. Res.*, *108*(A3), 1118, doi:10.1029/2002JA009758.

Ridley, A. J., and M. W. Liemohn (2002), A model-derived storm time asymmetric ring current driven electric field description, *J. Geophys. Res.*, *107*(A8), 1151, doi:10.1029/2001JA000051.

Sastri, J. H., M. A. Abdu, and J. H. A. Sobral (1997), Response of equatorial ionosphere to episodes of asymmetric ring current activity, *Ann. Geophys.*, *15*, 1316–1323, doi:10.1007/s00585-997-1316-3.

Sastri, J. H., N. Jyoti, V. V. Somayajulu, H. Chandra, and C. V. Devasia (2000), Ionospheric storm of early November 1993 in the Indian equatorial region, *J. Geophys. Res.*, *105*, 18,443–18,455, doi:10.1029/1999JA000372.

Sastri, J. H., K. Niranjan, and K. S. V. Subbarao (2002), Response of the equatorial ionosphere in the Indian (midnight) sector to the severe magnetic storm of July 15, 2000, *Geophys. Res. Lett.*, *29*(13), 1651, doi:10.1029/2002GL015133.

Scherliess, L., and B. Fejer (1997), Storm time dependence of equatorial disturbance dynamo zonal electric fields, *J. Geophys. Res.*, *102*, 24,037–24,046, doi:10.1029/97JA02165.

Siscoe, G. L., N. U. Crooker, and K. D. Siebert (2002), Transpolar potential saturation: Roles of region 1 current system and solar wind ram pressure, *J. Geophys. Res.*, *107*(A10), 1321, doi:10.1029/2001JA009176.

Spiro, R. W., R. A. Wolf, and B. G. Fejer (1988), Penetration of high-latitude electric fields effects to low latitudes during SUNDIAL 1984, *Ann. Geophys.*, *6*, 39–49.

Tsurutani, B., et al. (2004), Global dayside ionospheric uplift and enhancement associated with interplanetary electric field, *J. Geophys. Res.*, *109*, A08302, doi:10.1029/2003JA010342.

Wolf, R. A., R. W. Spiro, S. Sazykin, and F. R. Toffoletto (2007), How the Earth's inner magnetosphere works: An evolving picture, *J. Atmos. Sol. Terr. Phys.*, *69*, 288–302, doi:10.1016/j.jastp.2006.07.026.

S. Alex, Indian Institute of Geomagnetism, Navi Mumbai 410 206, India.

R. S. Dabas, National Physical Laboratory, New Delhi 110 012, India.

N. Dashora, National Atmospheric Research Laboratory, Gadanki 517 512, India.

P. Galav, R. Pandey, and S. Sharma, Department of Physics, Mohan Lal Sukhadia University, Udaipur 313 001, India. (pandey_r@yahoo.com)